ISSN: 2834-7706

Research Article

Journal of Mathematical Techniques and Computational Mathematics

Structural, Maorphological, Electrical and Optical Properties of SILAR Deposited Flowers Buds Like $SrMoO_4$ Film

M. R. Belkhedkar[1]*, P. R. Sonwane[2], P. D. Kundalwal[3], R. A. Tandan[4], G. A. Fedre[5], S. S. Umarkar[6], A.U. Ubale[7]

[1-6] Department of Physics, Shri Shivaji College of Arts, Commerce and Science, Akola 444003, Maharashtra, India.

[7]Nanostructured Thin Film Materials Laboratory, Department of Physics, Govt. Vidarbha Institute of Science and Humanities, VMV Road, Amravati 444604, Maharashtra, India.

***Corresponding Author:**
Department of Physics, Shri Shivaji College of Arts, Commerce and Science, Akola 444003, Maharashtra, India. mrbelkhedkar@yahoo.com

Submitted: 08 Dec 2022; **Accepted:**30 Dec 2022; **Published:**04 Jan 2023

Citation: Belkhedkar, M. R., Sonwane, P. R., Kundalwal, P. D., Tandan, R. A., Fedre, G. A., et al. (2023). Structural, Morphological, Electrical and Optical Properties of SILAR deposited flowers buds like SrMoO4 film. *J Math Techniques Comput Math,* 2(1), 01-06.

Abstract

Successive Ionic Layer Adsorption and Reaction (SILAR) method is employed to deposit microcrystalline flowers buds like $SrMoO_4$ film onto glass substrate using $SrCl_2.6H_2O$ and $Na_2MoO_4•2H_2O$ as cationic and anionic precursors respectively. Structural and morphological characterization of the film were carried out by means of X-ray diffraction, FTIR spectra, Field Emission Scanning Electron Microscopy and EDX studies, which confirms the formation of scheelite type tetragonal structure and flowers buds like microcrystalline grain growth of $SrMoO_4$ film. The optical band gap and activation energy of the $SrMoO_4$ film is found to be 3.6 and 1.15 eV respectively.

Keywords: Microcrystalline Materials; Electrical Properties; Optical Properties; X-ray Techniques, FTIR.

Introduction

In modern world, alkali earth metal molybdates such as $PbMoO_4$ [1], $NiMoO_4$ [2], $CaMoO_4$ [3], $BaMoO_4$ [4] and $SrMoO_4$ [5] plays a very important role in the fields of science and technology due to their novel physical and chemical properties [1-5]. Recently, alkali earth metal molybdates are the promising materials in view of its wide variety of applications such as luminescence materials, optical fibers, catalysis, scintillation detectors, optoelectronic devices, etc. [6]. Amongst the many metal molybdates, strontium molybdate ($SrMoO_4$) has attracted the attention of several researchers owing to its excellent luminescent and scintillation properties as well as thermal and chemical stability [7]. It has scheelite-type tetragonal crystal structure with oxyanion complex MoO_4^{2-} surrounded by eight Sr^{2+} cations [8]. Strontium molybdate exhibits n-type semiconducting character with direct band gap energy 3.7 eV [9].

It has variety of applications such as magnetic storage devices luminescent material white light emitting diode photocatalysts hydrogen sensor and biomedical materials as drug carrier etc. Recently, several researchers have been working on the deposition of strontium molybdate films by various methods such as cell electrochemical technique spray pyrolysis pulsed laser deposition chemical solution deposition method R. F. magnetron sputtering etc [10-19]. However, no report has been cited on the deposition of microcrystalline strontium molybdate films by successive ionic layer adsorption and reaction method. Successive Ionic Layer Adsorption and Reaction (SILAR) method was described by Nicolau in 1985[20]. It is one of the simple, safe, economical and ecofriendly chemical solution deposition method carried out at room temperature and under ambient pressure by utilizing the aqueous solutions. In SILAR, good quality films can be deposited simply by immersing the substrate into separately placed cationic and anionic precursors alternately, followed by the rinsing after each immersion to remove excess and loosely bound materials [21].

In the present investigation, an attempt has been made for the first time to deposit microcrystalline flower buds like SrMoO4 film onto glass substrate by successive ionic layer adsorption and reaction method. The structural, morphological, electrical and optical properties of as deposited $SrMoO_4$ film using XRD, FESEM, EDX, UV-Visible spectroscopy and two probe electrical resistivity measurement are reported.

Experimental

Successive ionic layer adsorption and reaction (SILAR) method is employed to grow microcrystalline strontium molybdate film onto glass substrate using 0.5M $SrCl_2.6H_2O$ and 0.2M $Na_2MoO_4•2H_2O$ as cationic and anionic precursors respectively. An analytical grade chemical is used as received without further purification [Loba Chemie Pvt. Ltd. Mumbai]. To achieve uniform deposition of the film, all the glassware and substrates were thoroughly cleaned by usual cleaning method. Several trials have been made by varying the preparative parameters like concentration, pH, immersion time, deposition cycles etc. The optimized preparative parameters are shown in

Table.1. Initially, the well cleaned glass substrate is immersed in cationic precursor solution for 20s, where it adsorbs Sr^{2+} species on substrate surface. Further the substrate is rinsed into the de-ionized water for 20s to remove loosely bound Sr^{2+} species from the substrate surface. Afterwards, the substrate is immersed into the anionic precursor solution for 20s, where Sr^{2+} ions react with MoO_4^{2-} ions and forms a layer of $SrMoO_4$. Further the glass substrate is rinsed into the de-ionized water to remove unreacted species and loosely bound material from the substrate surface. This completes one SILAR deposition cycle. By repeating 50 such SILAR cycles pale greenish colored $SrMoO_4$ film of terminal thickness 548 nm was obtained. The as deposited film was dried at room temperature and annealed in the muffle furnace at 773K for 2h to obtain metallic grey colored pure phase $SrMoO_4$.

In the present work, film thickness was measured by gravimetric weight difference method with bulk density of deposited material ($SrMoO_4$ = 4.68 gcm-3) [21, 22]. The structural characterization of strontium molybdate film was carried out by analyzing the X-ray diffraction pattern obtained with Xpert PRO PANalytical diffractometer with monochromatized Cu Kα radiation of wavelength 0.154 nm. The FTIR spectrum of the sample was collected using a Shimadzu IR Affinity-I make FTIR unit. The film morphology was observed by field emission scanning electron microscopy (FE-SEM) and energy dispersive X-ray spectroscopy (EDX) (Model: MERLIN). The optical absorption studies were carried out within the wavelength range 300 – 750 nm using ELICO ® Double Beam SL 210 UV-Visible Spectrophotometer. The variation of electrical resistivity of $SrMoO_4$ film with temperature was studied by using two probe method.

Table 1: Optimized preparative parameters for the deposition of $SrMoO_4$ film.

Deposition conditions	Cationic precursor	Anionic precursor
Precursors	SrCl2.6H2O	Na2MoO4•2H2O
Concentrations (mol/L)	0.5	0.2
pH	1	8
Immersion time (s)	20	20
Temperature (K)	303	303
No. of SILAR Cycles	50	50
Volume of precursor (ml)	50	50

Results and discussion

Film Formation Mechanism

Microcrystalline $SrMoO_4$ film was prepared by using SILAR method onto glass substrates by immersing the glass substrate into separately placed cationic and anionic precursors. The deposition mechanism involves the ion-by-ion growth process at nucleation sites on the immersed surfaces is as follow. In aqueous solution $SrCl_2$ dissociates as,

$$SrCl_2 \rightarrow Sr^{2+} + 2Cl^- \quad (1)$$

Similarly, in aqueous solution Na_2MoO_4 dissociates as,

$$Na_2MoO_4 \rightarrow 2Na^+ + MoO_4^{2-} \quad (2)$$

When substrate is immersed in $SrCl^2$ precursor, Sr^{2+} ions get adsorbed on the substrate surface. These Sr^{2+} ions during further immersion react with the MoO_4^{2-} ions present in Na_2MoO_4 precursor. This results in the formation of well adherent and uniform $SrMoO_4$ film [15].

$$Sr^{2+} + MoO_4^{2-} \leftrightarrow SrMoO_4 \quad (3)$$

Structural Studies

The phase and crystal structure of the strontium molybdate film was studied by X-ray diffraction carried out at 2θ degree in the range 20 - 80 degree. The X-ray diffraction pattern of strontium molybdate film of thickness 548 nm is shown in Fig.3.1. The (1 1 2), (0 0 4), (2 0 0), (1 1 4), (2 0 4), (2 2 0), (1 1 6), (3 1 2), (2 2 4) and (3 1 6) peak observed in the X-ray diffraction pattern are due to scheelite type tetragonal crystal structure of strontium molybdate ($SrMoO_4$) with space group I41/a in comparison with the standard X-ray diffraction data card [JCPDS: 08-0482]

Table.2. The scheelite type tetragonal crystal structure of $SrMoO_4$ may formed due to an oxyanion complex MoO_4^{2-} surrounded by eight Sr^{2+} cations.

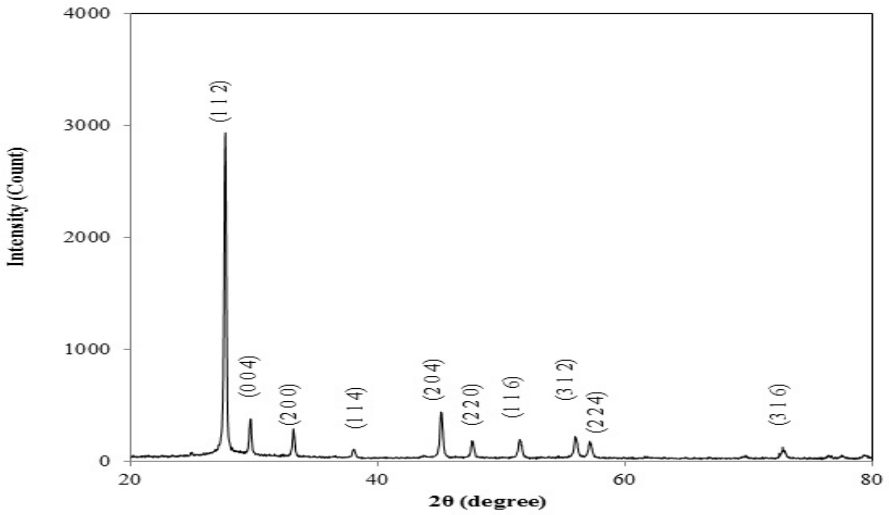

Figure 1: X-ray diffraction pattern of $SrMoO_4$ film deposited onto glass substrate.

Table 2: Comparison of observed X-ray diffraction data in accordance with JCPDS data card 08-0482.

h k l	Standard data		Observed data	
	d value	2θ(degree)	d value	2θ (degree)
1 1 2	3.2220	27.662	3.2247	27.640
0 0 4	3.0060	29.694	3.0075	29.680
2 0 0	2.6980	33.176	2.7010	33.140
1 1 4	2.3610	38.065	2.3636	38.040
2 0 4	2.0080	45.113	2.0095	45.080
2 2 0	1.9070	47.645	1.9088	47.600
1 1 6	1.7740	51.467	1.7749	51.440
3 1 2	1.6420	55.951	1.6418	55.960
2 2 4	1.6110	57.125	1.6112	57.120
3 1 6	1.2994	72.708	1.2993	72.720

FTIR Study

A typical FTIR spectrum of the $SrMoO_4$ film of thickness 548 nm in the mid-infrared frequency range from 400 to 4000 cm^{-1} is shown in Fig. 2. The peaks observed in the FTIR spectra at 439.77 cm^{-1} may correspond to the asymmetric vibration frequencies of Sr - O bond [24]. However, absorption peak observed at, 418.11 may be due to Mo-O bending vibration mode and 839.03 cm^{-1} may correspond to Mo-O stretched vibration mode [9]. In addition, peaks observed in the spectra at 143.5.04, 1627.92, 2343.51 and 3342.64 cm^{-1} may originate due to the presence of OH after absorption of moisture from atmosphere and impurity from KBr during sample preparation.

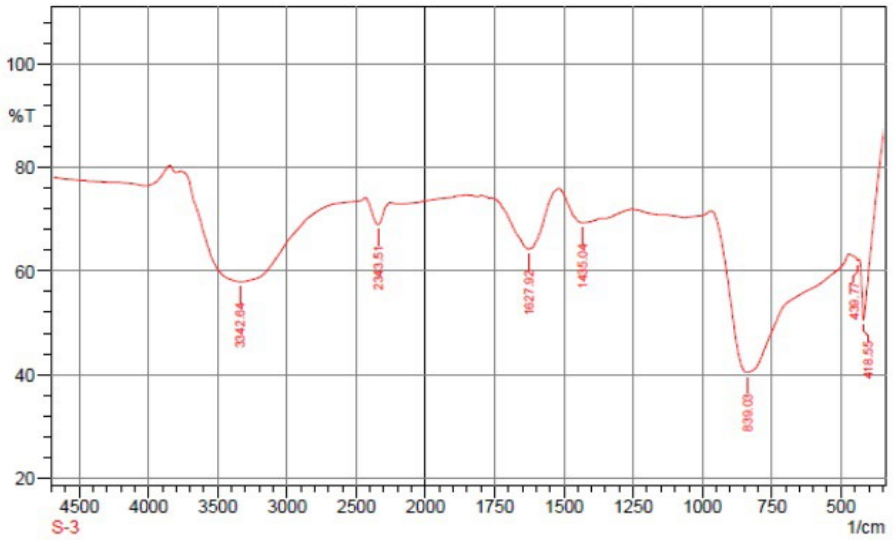

Figure 2: FTIR spectrum of $SrMoO_4$ film.

Surface morphology

Surface morphology of the strontium molybdate ($SrMoO_4$) film was examined by using FESEM (Fig.3A). The FESEM micrograph reveals the flower buds like microstructural grain growth of strontium molybdate uniformly distributed over the substrate surface. It is clearly seen that these structures are constituted from nano particles of $SrMoO_4$ which are overlapping each other to form seed particles. These seed particles due to large surface free energy agglomerate faster and grow into larger grain to form flower buds like $SrMoO_4$ structures. The flower buds like morphology of the film is in good agreement with X-ray diffraction results. The elemental analysis of the strontium molybdate film was carried out using energy dispersive X-ray (EDX) analysis (Fig. 3B). The elemental analysis carried only for Sr, M and O elements. The elemental peaks present in the EDAX spectra reveal the formation of $SrMoO_4$.

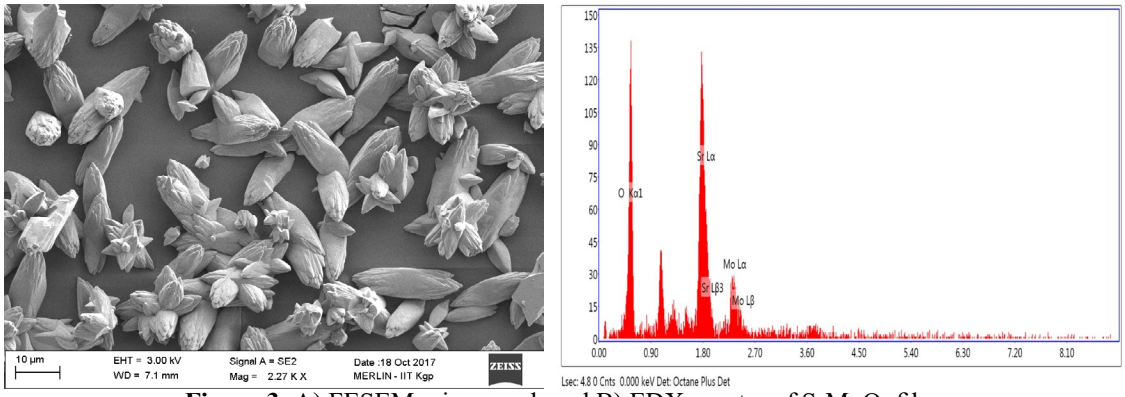

Figure 3: A) FESEM micrograph and B) EDX spectra of $SrMoO_4$ film.

Optical Studies

The optical absorption spectrum of $SrMoO_4$ film was studied in the range of wavelength 300 - 750 nm at room temperature (inset of Figure 4.). The maximum absorption in the visible region shows that the strontium molybdate film can be used as absorber in the visible region for the optoelectronic devices. The optical band gap (Eg) of $SrMoO_4$ film was calculated using the following equation,

$$\alpha h\upsilon = A(Eg - h\upsilon)^n \quad (4)$$

where, 'α' is absorption coefficient, 'Eg' is band gap, 'A' is constant and n is equal to 1/2 for indirect and 2 for direct transition [25]. The plot of (α hυ) 2 versus hυ of $SrMoO_4$ film is shown

Figure 4. The direct band gap energy was estimated by extrapolating the linear portion of the plot to the energy axis at (α hυ) 2 = 0. The optical band gap energy of $SrMoO_4$ film deposited by SILAR method was found to be 3.6 eV which is smaller than the earlier report [9, 13]. This decrease in the value of band gap energy may due to increase in thickness of $SrMoO_4$ film. As the film thickness increases, localized states within the band gap increases which further decrease the band gap energy of the film [26].

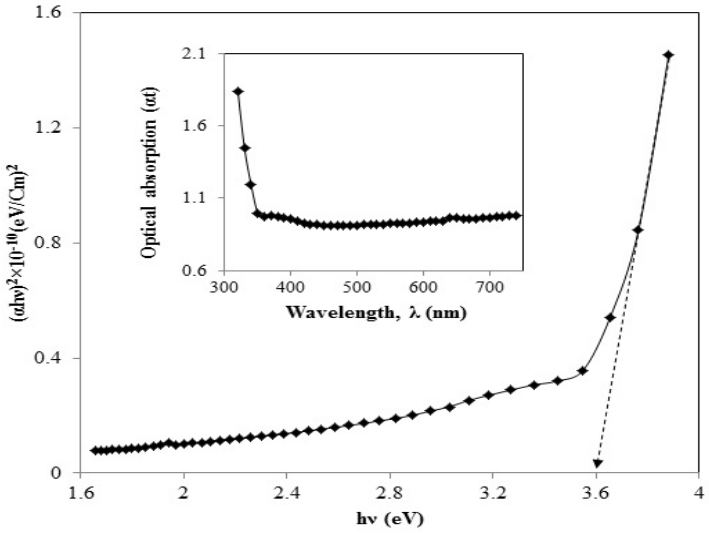

Figure 4: The plot of $(\alpha h\nu)^2$ versus hν (Inset shows optical absorption spectra) of $SrMoO_4$ film.

Electrical resistivity

The D.C two-point probe method (with silver paste contact) was employed to understand the variation of electrical resistivity of $SrMoO_4$ film with temperature (Figure 5). The decrease in electrical resistivity with increase in temperature indicates semiconducting behavior of $SrMoO_4$. The electrical resistivity of the $SrMoO_4$ film at room temperature is found to be 11×10^7 Ωcm. The activation energy was calculated by using the relation,

$$\rho = \rho_o(E_a/KT) \qquad (5)$$

where 'ρ' is the resistivity at temperature T, 'ρ0' is constant; 'K' is Boltzmann constant and 'Ea' is activation energy [27]. The activation energy of $SrMoO_4$ film deposited onto glass substrate was found to be 1.15 eV.

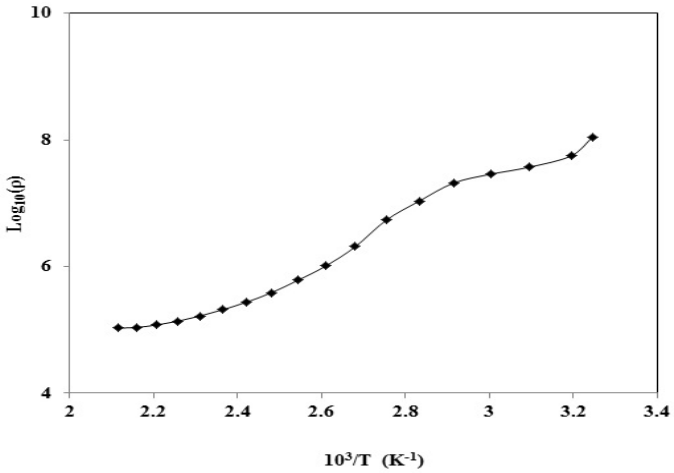

Figure 5: The plot of log ρ versus 10^3/ T of $SrMoO_4$ film.

Conclusions

In present work, microcrystalline $SrMoO_4$ film was successfully grown by Successive Ionic Layer Adsorption and Reaction (SILAR) method onto glass substrate. The X-ray diffraction and FTIR study reveals the formation of scheelite type tetragonal strontium molybdate ($SrMoO_4$) with space group I41/a. However, a FESEM and EDX characterization confirms the microstructural flowers buds like grain growth of $SrMoO_4$. The direct optical band gap energy and activation energy of the $SrMoO_4$ film are found to be 3.6 and 1.15 eV respectively.

Acknowledgment

Authors are thankful to Principal, Shri Shivaji College of Arts, Commerce and Science, Akola for providing all the necessary research facility.

References

1. Hernandez-Uresti, D. B., Martínez-de la Cruz, A., & Tor-

res-Martínez, L. M. (2016). Photocatalytic degradation of organic compounds by $PbMoO_4$ synthesized by a microwave-assisted solvothermal method. Ceramics International, 42(2), 3096-3103.
2. Yin, Z., Zhang, S., Chen, Y., Gao, P., Zhu, C., Yang, P., & Qi, L. (2015). Hierarchical nanosheet-based NiMoO 4 nanotubes: synthesis and high supercapacitor performance. Journal of Materials Chemistry A, 3(2), 739-745.
3. Gupta, S. K., Sahu, M., Ghosh, P. S., Tyagi, D., Saxena, M. K., & Kadam, R. M. (2015). Energy transfer dynamics and luminescence properties of Eu^{3+} in $CaMoO_4$ and $SrMoO_4$. Dalton Transactions, 44(43), 18957-18969.
4. Jena, P., Gupta, S. K., Natarajan, V., Sahu, M., Satyanarayana, N., & Venkateswarlu, M. (2015). Structural characterization and photoluminescence properties of sol–gel derived nanocrystalline BaMoO4: Dy3+. Journal of Luminescence, 158, 203-210.
5. Du, P., & Yu, J. S. (2015). Dual-enhancement of photoluminescence and cathodoluminescence in Eu 3+-activated $SrMoO_4$ phosphors by Na+ doping. RSC Advances, 5(74), 60121-60127.
6. Ren, X., Zhang, Y., Li, Q., & Yu, M. (2014). Sodium citrate (Na3Cit)-assisted hydrothermal synthesis of uniform spindle-like $SrMoO_4$: Eu^{3+} phosphors. Materials Research Bulletin, 59, 283-289.
7. Jiang, H., Rooh, G., Kim, H. J., Park, H., So, J. H., Kim, S., ... & Zhang, W. (2013). Growth and scintillation characterizations of $SrMoO_4$ single crystals. Journal of the Korean Physical Society, 63(10), 2018-2023.
8. Nogueira, I. C., Cavalcante, L. S., Pereira, P. F. S., De Jesus, M. M., Rivas Mercury, J. M., Batista, N. C., ... & Longo, E. (2013). Rietveld refinement, morphology and optical properties of $(Ba_{1-x}Sr_x)$ MoO_4 crystals. Journal of Applied Crystallography, 46(5), 1434-1446.
9. Vidya, S., John, A., Solomon, S., & Thomas, J. K. (2012). Optical and dielectric properties of $SrMoO_4$ powders prepared by the combustion synthesis method. Advances in materials Research, 1(3), 191.
10. Hu, L., Lin, G. T., Wei, R. H., Luo, X., Tang, X. W., Zhu, X. B., ... & Sun, Y. P. (2017). Unipolar resistive switching behavior of amorphous $SrMoO_4$ thin films deposited at room temperature. Ceramics International, 43(3), 3177-3182.
11. Tang, X., Zhu, X., Dai, J., Yang, J., Hu, L., Chen, L., ... & Sun, Y. (2014). c-Axis oriented $SrMoO_4$ thin films by chemical solution deposition: self-assembled orientation, grain growth and photoluminescence properties. Acta materialia, 65, 287-294.
12. Shivakumara, C., & Saraf, R. (2015). Eu3+-activated $SrMoO_4$ phosphors for white LEDs applications: Synthesis and structural characterization. Optical Materials, 42, 178-186.
13. Ciftyürek, E., Sabolsky, K., & Sabolsky, E. M. (2017). High temperature selective sensing of hydrogen with MgO-modified $SrMoO_4$ micro-fibers. Sensors and Actuators B: Chemical, 249, 296-310.
14. Wang, Y., Yang, P., Qu, F., Gai, S., Niu, N., He, F., & Lin, J. (2013). Hollow structured $SrMoO_4$: Yb^{3+}, Ln^{3+} (Ln= Tm, Ho, Tm/Ho) microspheres: tunable up-conversion emissions and application as drug carriers. Journal of Materials Chemistry B, 1(15), 2056-2065.
15. Chen, L., & Gao, Y. (2007). Mechanisms and applications of cell electrochemical technique to prepare luminescent $SrMoO_4$ thin films. Chemical Engineering Journal, 131(1-3), 181-185.
16. Lou, Z., & Cocivera, M. (2002). Cathodoluminescence of $CaWO_4$ and $SrWO_4$ thin films prepared by spray pyrolysis. Materials research bulletin, 37(9), 1573-1582.
17. Huang, J. Y., & Jia, Q. X. (2003). Structural properties of $SrWO_4$ films synthesized by pulsed-laser deposition. Thin Solid Films, 444(1-2), 95-98.
18. Lei, H., Zhu, X., Sun, Y., & Song, W. (2008). Preparation of $SrMoO_4$ thin films on Si substrates by chemical solution deposition. Journal of crystal growth, 310(4), 789-793.
19. Cho, S. (2017). Optical and structural properties of Sm-doped $SrMoO_4$ phosphor thin films deposited on sapphire substrates. Journal of the Korean Physical Society, 71(12), 1006-1011.
20. Nicolau, Y. F. (1985). Solution deposition of thin solid compound films by a successive ionic-layer adsorption and reaction process. Applications of Surface Science, 22, 1061-1074.
21. Ubale, A. U., & Belkhedkar, M. R. (2015). Size dependent physical properties of nanostructured α-Fe_2O_3 thin films grown by successive ionic layer adsorption and reaction method for antibacterial application. Journal of Materials Science & Technology, 31(1), 1-9.
22. Li, Z., Wang, J., Zhang, H., Yu, H., & Pan, Z. (2011). Growth and characterization of large $SrMoO_4$ crystals. Journal of crystal growth, 318(1), 679-682.
23. Ubale, A. U., Sakhare, Y. S., Bhute, M. V., Belkhedkar, M. R., & Singh, A. (2013). Size-dependent structural, electrical and optical properties of nanostructured iron selenide thin films deposited by Chemical Bath Deposition Method. Solid state sciences, 16, 134-142.
24. Athar, T. (2013). Synthesis and characterization of strontium oxide nanoparticles via wet process. Materials Focus, 2(6), 450-453.
25. Mahdi, M. A., Hassan, J. J., Hassan, Z., & Ng, S. S. (2012). Growth and characterization of $Zn_xCd_{1-x}S$ nanoflowers by microwave-assisted chemical bath deposition. Journal of Alloys and Compounds, 541, 227-233.
26. El-Zahed, H., Dongol, M., & Radwan, M. (2002). Annealing and thickness effect on the optical absorption of $Ge_{20}Te_{80}$ and $Cu_6Ge_{14}Te_{80}$ films. The European Physical Journal-Applied Physics, 17(3), 179-186.
27. Belkhedkar, M. R., & Ubale, A. U. (2016). Physical properties of Fe doped Mn3O4 thin films synthesized by SILAR method and their antibacterial performance against E. coli. Journal of Saudi Chemical Society, 20(5), 553-560.